



EFFICIENT CONCENTRATION OF PB FROM WATER BY REACTIONS WITH LAYERED ALKALI SILICATES, MAGADIITE AND OCTOSILICATE

DONHATAI SRUAMSIRI¹, THIPWIPA SIRINAKORN², AND MAKOTO OGAWA¹*

¹School of Energy Science and Engineering, Vidyasirimedhi Institute of Science and Technology (VISTEC), 555 Moo 1 Payupnai, Wangchan, Rayong 21210, Thailand

²School of Molecular Science and Engineering, Vidyasirimedhi Institute of Science and Technology (VISTEC), 555 Moo 1 Payupnai, Wangchan, Rayong 21210, Thailand

Abstract—Human health problems are often related to contamination of the aqueous environment by toxic metal ions. In the present study, two layered alkali silicates (magadiite and octosilicate) were examined to assess removal of Pb^{2+} from aqueous solutions in terms of quantity and kinetics. The ion-exchange reaction between the silicates and aqueous solutions of lead(II) acetate at various concentrations was examined at room temperature for 24 h. The adsorption isotherms were H-type, showing the strong interactions between Pb^{2+} and the silicates. The amounts of Pb^{2+} adsorbed were as much as 1.23 mmol Pb/g magadiite and 2.32 mmol Pb/g octosilicate, which are larger than the reported values for various ion exchangers. They were larger than the theoretical cation exchange capacities (2.2 and 3.7 meq/g for magadiite and octosilicate, respectively), suggesting that the collection of Pb^{2+} included the precipitation as basic lead salts in addition to the ion exchange. The adsorption isotherms for magadiite and octosilicate fitted the Langmuir equation with correlation coefficients, R^2 , of 0.9991 and 0.9972, respectively. The adsorption of Pb^{2+} onto the layered alkali silicates from acidic aqueous solution was examined to obtain smaller amounts of adsorbed Pb^{2+} (0.32 mmol Pb/g magadiite and 0.34 mmol Pb/g octosilicate), confirming the important role of pH on the surface charge of the layered silicates in terms of ion exchange. The adsorption of Pb^{2+} reached equilibrium within 5 min for magadiite while it took 60 min for octosilicate. The difference was in the particle morphology; smoother diffusion of Pb^{2+} was possible through flower-shaped aggregates of particles of magadiite.

Keywords—Layered alkali silicate · Magadiite · Octosilicate · Pb^{2+} collection · Water purification

INTRODUCTION

Collection of metal ions from aqueous environments has been investigated to concentrate useful metal ions from nature and waste and to remove toxic metal ions as part of the remediation of contaminated water. In addition to membrane separation and precipitation for the collection of target metals (Divrikli et al., 2007; Chen et al., 2009; Jiang et al., 2011), adsorption onto solids (adsorbents) is another useful way to collect metal ions and metal oxo ions from aqueous environments (Li et al., 2002; Dabrowski et al., 2004; Guerra et al., 2010; Benkhatou et al., 2016; Attar et al., 2019). Various natural and synthetic ion exchangers are available for a variety of target ions to be collected. Parameters such as adsorbent–adsorbate interactions for adsorption from low concentration, capacity of the adsorption, and kinetics have been examined to find suitable adsorbents and conditions.

Some inorganic layered solids are known as ion exchangers, and they are characterized by greater chemical and thermal stabilities over organic and polymeric ion exchangers (Clearfield, 1996). Ion-exchangeable layered solids such as the

smectite group of clay minerals (Okada et al., 2014; Otunola and Oloade, 2020), layered alkali silicates (Murakami et al., 2006; Homhuan et al., 2017b; Sirinakorn et al., 2018a), layered alkali titanates (Komatsu et al., 1982; Ide et al., 2014), and layered double hydroxides (Miyata, 1983; Kaneko & Ogawa, 2013; Mandel et al., 2013; Selvam et al., 2014), are non-toxic and environmentally friendly adsorbents. Layered solids with various ion-exchange capacities are known, while the experimentally determined amounts of ions collected are not always consistent with the cation exchange capacities (CECs), which are derived from the chemical formula, probably due to the stability of the adsorbents, the pH dependence of the ion exchange sites, etc. The kinetics of the ion exchange and the ion selectivity have also been investigated (Googerdchian et al., 2012; Liu et al., 2016; Mousa et al., 2016; Hong et al., 2020).

Layered alkali silicates such as kanemite, makatite, octosilicate, magadiite, and kenyaite are composed of silicate sheets and charge-neutralizing alkali cations in the interlayer space (Schwieger et al., 2004; Selvam et al., 2014). The theoretical CEC values (derived from the chemical formulae) of magadiite and octosilicate are 2.2 and 3.7 meq/g (Lagaly et al., 1975; Selvam et al., 2014), which are large if compared with conventional inorganic ion exchangers such as zeolites and bentonite (~1.0 meq/g) (Auerbach et al., 2004). The collection of Zn^{2+} (Hatsushika, 1996; Murakami et al., 2006; Ide et al., 2011), Co^{2+} (Hatsushika, 1996; Ogawa and Takahashi, 2007), Cu^{2+} (Murakami et al., 2006; Mokhtar et al., 2018), In^{3+} (Homhuan et al., 2017a), Eu^{3+} (Mizukami et al., 2002), and As^{3+} (Guerra et al., 2008) by magadiite has been reported

This paper is based on a presentation made during the 4th Asian Clay Conference, Thailand, June 2020.

* E-mail address of corresponding author: waseda.ogawa@gmail.com

DOI: 10.1007/s42860-021-00140-x

© The Clay Minerals Society 2021

previously, while few reports exist on the ion exchange of octosilicate. Thus, in the present study, layered alkali silicates (magadiite and octosilicate) were examined for their ability to remove Pb^{2+} from aqueous solution. In addition, the kinetic aspects of Pb^{2+} adsorption on the various particle morphologies of layered alkali silicates (magadiite and octosilicate) were also investigated.

EXPERIMENTAL

Materials

Silica gel ($\text{SiO}_2 \cdot 0.002\text{H}_2\text{O}$, silica gel 60, particle size of 0.063–0.100 mm, Merck KGaA, Darmstadt, Germany), sodium hydroxide pellets (NaOH >97%, Ajax Finechem, New South Wales, Australia), lead(II) acetate trihydrate ($(\text{CH}_3\text{COO})_2\text{Pb} \cdot 3\text{H}_2\text{O}$, abbreviated as $\text{Pb}(\text{ac})_2$, >99.5%, Merck KGaA, Darmstadt, Germany), and aqueous HNO_3 solution (65%, Merck KGaA, Darmstadt, Germany) were used without further purification. Milli-Q water (ELGA, model: OS007BPM1, Type II $15 \text{ M}\Omega \cdot \text{cm}$, High Wycombe, UK) was used throughout.

Preparation of Magadiite and Octosilicate

Na-magadiite was prepared by the hydrothermal reaction of NaOH and SiO_2 as reported previously (Kosuge et al., 1992; Ide & Ogawa, 2007). NaOH (4.14 g) was dissolved in water (150 mL) and 28.4 g of silica gel was added to the NaOH solution. The gel was stirred for 1 h at room temperature. The mixture was sealed in a Teflon-lined stainless steel bottle and treated hydrothermally at 150°C for 2 days. The product was collected by centrifugation, washed with a dilute aqueous solution of NaOH (pH 10.0), and dried in air at 40°C for 2 days. Na-octosilicate was prepared by a hydrothermal reaction as reported previously (Endo et al., 1994). NaOH (25.8 g) was dissolved in water (150 mL) and 81.5 g of silica gel was added to the NaOH solution. The gel was stirred for 1 h at room temperature. The mixture was sealed in a Teflon-lined stainless steel bottle and treated hydrothermally at 100°C for 1 month. The product was collected by centrifugation and dried in air at 40°C for 2 days.

Adsorption of Pb^{2+} from Aqueous Solution

Adsorption of Pb^{2+} onto the layered alkali silicates was examined by means of the reaction between the layered alkali silicates and aqueous solution of $\text{Pb}(\text{ac})_2$. A layered alkali silicate (0.1 g) was dispersed in water (25 mL) and stirred magnetically for 1 h. An aqueous solution of $\text{Pb}(\text{ac})_2$ (25 mL) was mixed with the aqueous suspension of the layered alkali silicates and the mixture was stirred magnetically at room temperature for 24 h. The initial concentration of Pb^{2+} was 0.2, 0.6, 1.0, 2.2, 2.8, 3.6, and 4.0 mM for magadiite and 0.2, 0.6, 1.0, 3.7, 4.0, 5.0, and 6.0 mM for octosilicate. The solids were collected by centrifugation using models CR22N and R20A2 rotors, from Hitachi Koki (Tokyo, Japan) at 20,000 rpm ($48,000 \times g$) for 10 min and dried in air at 40°C for 2 days. The concentration of Pb^{2+} in the supernatant was determined by inductively coupled plasma-optical emission spectroscopy (ICP-OES), from Agilent Technologies 700 Series instrument (California, USA). Adsorption of Pb^{2+} onto the layered alkali silicates from acidic

aqueous solution was also examined using the aqueous solution of the $\text{Pb}(\text{ac})_2$ (3.7 mM and pH = 2, which was adjusted by the addition of HNO_3 solution).

The ion-exchange reactions were performed by varying reaction times (2, 5, 10, 30, 60, 120, and 180 min) in order to follow Pb^{2+} adsorption kinetics by the following condition: a layered alkali silicate (0.1 g) was dispersed in water (25 mL) and stirred magnetically for 1 h. $\text{Pb}(\text{ac})_2$ solution (25 mL, 2.2 mM for magadiite and 3.7 mM for octosilicate) was added into the suspension. The solids were collected by centrifugation using models CR22N and R20A2 rotors, Hitachi Koki (Tokyo, Japan) at 20,000 rpm ($48,000 \times g$) for 10 min after mixing for various times (2, 5, 10, 30, 60, 120 and 180 min) at room temperature. The concentration of Pb^{2+} in the supernatant was determined by ICP-OES.

Characterization

X-ray powder diffraction (XRD) patterns were recorded on a Bruker (Karlsruhe, Germany) NEW D8 ADVANCE X-ray powder diffractometer using Ni-filtered $\text{CuK}\alpha$ irradiation operated at 40 kV and 40 mA. Inductively coupled plasma-optical emission spectroscopy (ICP-OES) was performed on an Agilent Technologies (California, USA) 700 Series instrument. Calibration curves (R factor > 0.99) were made for each measurement using standard $\text{Pb}(\text{ac})_2$ solution. Scanning electron microscopy (SEM) was done using a JEOL (Tokyo, Japan) JSM-7610F scanning electron microscope for samples coated with Pt. Elemental mapping was obtained using an energy dispersive X-ray fluorescence spectrometer (X-Max 150 mm^2 , Oxford, UK) attached to the SEM.

RESULTS AND DISCUSSION

Preparation of Magadiite and Octosilicate

The formation of magadiite and octosilicate (Kosuge et al., 1992; Endo et al., 1994; Ide & Ogawa, 2007) was confirmed by the XRD patterns (Figs. 1a and 2a) and SEM images (Figs. 3a and 4a).

Adsorption of Pb^{2+} on Magadiite and Octosilicate

The XRD patterns of magadiite and octosilicate after reaction with Pb^{2+} are shown in Figs. 1 and 2. The basal spacing (d_{001}) of magadiite decreased from 1.57 nm to 1.42 nm after the reaction with Pb^{2+} , suggesting ion exchange between Pb^{2+} and Na in the interlayer space. The intensity of the d_{001} reflection became weaker after the adsorption of Pb^{2+} . The interlayer space was calculated from the observed basal spacing (1.42 nm) by subtracting the thickness of the silica layer of magadiite, which was estimated from the basal spacing of the H-magadiite (Rojo et al. 1988), to be 0.30 nm, thus giving a final value of 1.12 nm. The observed basal spacing (1.42 nm) was similar to that (1.43 nm) reported for the Pb^{2+} -exchanged magadiite (Hatsushika, 1996). The basal spacing (d_{001}) of octosilicate decreased from 1.10 nm to 0.88 nm after reaction with Pb^{2+} , suggesting ion exchange between Na and Pb^{2+} in the interlayer space. Because the thickness of the silicate layer of octosilicate is 0.74 nm (Vortmann et al., 1997), the

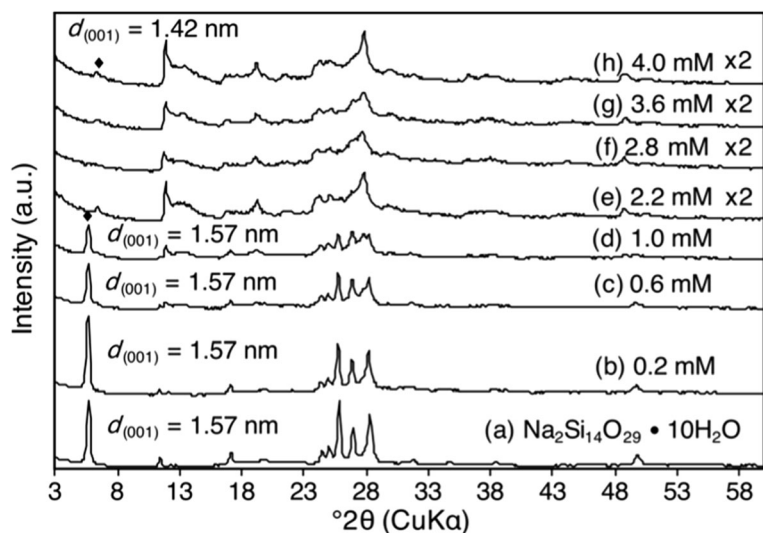


Fig. 1 XRD patterns of magadiite: **a** before and **b–h** after the reactions with initial aqueous solutions of $\text{Pb}(\text{ac})_2$ of **b** 0.2, **c** 0.6, **d** 1.0, **e** 2.2, **f** 2.8, **g** 3.6, and **h** 4.0 mM

interlayer space of the Pb^{2+} -adsorbed octosilicate was estimated (by subtracting the thickness of the silicate layer from the observed basal spacing) to be 0.14 nm. The observed basal spacing (0.88 nm) is consistent with the value (0.85 nm) reported for Pb^{2+} exchanged octosilicate (Lim et al., 2017). Those authors reported that the shrinkage of the basal spacing was caused by dehydration after the adsorption of Pb^{2+} . The difference in the interlayer spaces for Pb^{2+} adsorbed magadiite (0.30 nm) and octosilicate (0.14 nm) in the present study was due to the difference in the hydration of the interlayer Pb^{2+} as well as the silicate framework deterioration.

The SEM images and elemental mapping of magadiite (Fig. 3) and octosilicate (Fig. 4) before and after reaction with the aqueous solution of $\text{Pb}(\text{ac})_2$ (the initial concentration of

4.0 mM for magadiite and 6.0 mM of octosilicate) revealed that, even though the XRD peaks became weaker after the reaction with Pb^{2+} (Figs. 1 and 2), the flower-shaped morphology (4–5 μm) of magadiite composed of aggregated platy particles (1–2 μm) and the platy morphology of octosilicate (2–4 μm) were retained. Pb^{2+} was distributed homogeneously in/on the silicate particles for both magadiite (Fig. 3) and octosilicate (Fig. 4) systems, confirming the successful ion exchange.

Adsorption Isotherm of Pb^{2+} on Magadiite and Octosilicate

The adsorption isotherms of Pb^{2+} on magadiite and octosilicate (Fig. 5) were of type H, according to the classification by Giles et al. (1960), suggesting significant affinity

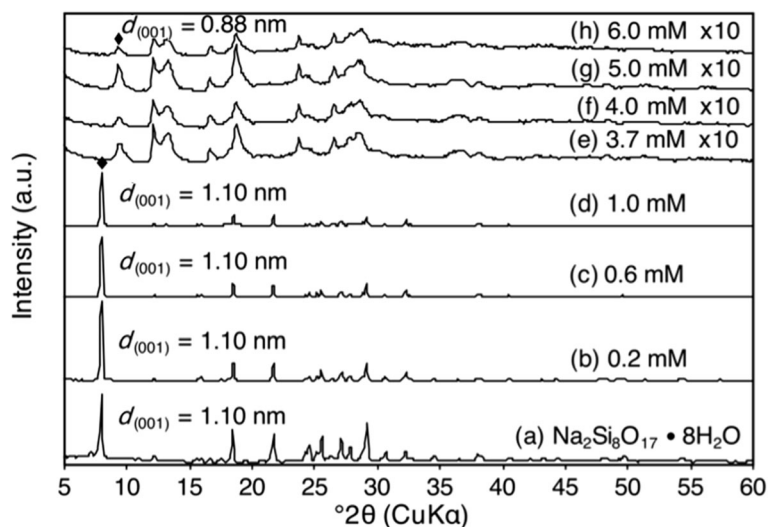


Fig. 2 XRD patterns of octosilicate: **a** before and **b–h** after the reaction the with initial aqueous solutions of $\text{Pb}(\text{ac})_2$ of **b** 0.2, **c** 0.6, **d** 1.0, **e** 3.7, **f** 4.0, **g** 5.0, and **h** 6.0 mM

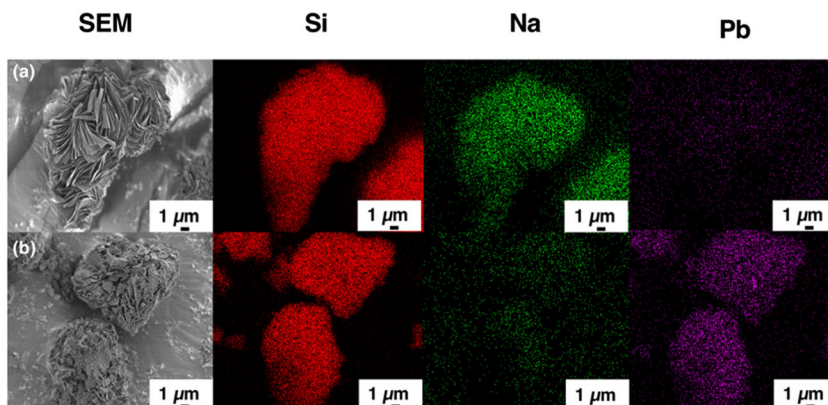


Fig. 3 SEM images and elemental mapping of magadiite: **a** before and **b** after the reaction with a $\text{Pb}(\text{ac})_2$ solution concentration of 4.0 mM

between Pb^{2+} and the layered alkali silicates. The ideal cation exchange capacities of magadiite (2.2 meq/g) and octosilicate (3.7 meq/g), which are derived from the chemical formulae (magadiite, $\text{Na}_2\text{Si}_{14}\text{O}_{29}\cdot 10\text{H}_2\text{O}$, and octosilicate, $\text{Na}_2\text{Si}_8\text{O}_{17}\cdot 8\text{H}_2\text{O}$), are shown by the dotted lines (Fig. 5) to confirm that the amounts of Pb^{2+} adsorbed were larger than the calculated CEC values, especially for octosilicate. The adsorption of Pb^{2+} on magadiite reached the theoretical CEC value (2.2 meq/g) when the initial concentration of $\text{Pb}(\text{ac})_2$ was 2.2 mM. When solutions of higher concentrations (2.8, 3.6, 4.0 mM) were used, the amounts of Pb^{2+} adsorbed were slightly more than the theoretical CEC value (2.2 meq/g) and the maximum amount of Pb^{2+} adsorbed was 1.27 mmol Pb/g magadiite (initial pH = 6.0). The adsorption of Pb^{2+} on octosilicate reached the theoretical CEC value (3.7 meq/g) when the initial concentration of $\text{Pb}(\text{ac})_2$ was 3.7 mM. When solutions of greater concentrations (4.0, 5.0, 6.0 mM) were used, the amounts of Pb^{2+} adsorbed were greater than the theoretical CEC (3.7 meq/g) and the maximum was 2.34 mmol Pb/g octosilicate (initial pH = 6.0).

The reported collection of Pb^{2+} from aqueous solution by means of ion exchangers such as Na-bentonite (Glatstein & Francisca, 2015), carbon nanotubes (Li et al., 2002; Abbas et al., 2016; Aliyu et al., 2017), activated carbon (Goel et al., 2005; Chen et al., 2014), fly ash (Al-Zboon et al., 2011;

Barbosa et al., 2014), zeolite (Jamil et al., 2010), and natural apatite (Kaludjerovic-Radoicic & Raicevic, 2010) is summarized in Table 1. The amounts of Pb^{2+} adsorbed by magadiite (1.27 mmol/g) and octosilicate (2.34 mmol/g) in the present study were greater than those reported for other adsorbents (Table 1), confirming the advantages of using magadiite and, in particular, octosilicate, as very high-capacity adsorbents of Pb^{2+} .

Literature reports of the amount of Pb^{2+} adsorbed by magadiite vary widely (Table 1). Benkhatou et al. (2016) reported 0.048 mmol Pb/g (initial pH = 7.0), whereas Lim et al. (2017) reported that the adsorption of Pb^{2+} from aqueous NaCl solution could reach as high as 0.97 mmol Pb/g magadiite and 1.5 mmol Pb/g octosilicate. The experimental conditions (pH, Pb^{2+} concentration, presence of competing ions, as well as the amount of adsorbent) may account for this difference. Because the negative charge of the layered alkali silicates is pH dependent (Schwieger et al., 2004), protons may compete with Pb^{2+} for the exchange with Na at lower pH. For example, in the present study, the initial pH of the $\text{Pb}(\text{ac})_2$ solution was in the range 5.9–6.0 and that of the silicate suspension was in the range 9.5–10.0. After mixing the solution and the suspension, the pH of the mixture was in the range 6.1–8.8 for the magadiite system and 6.6–9.3 for the octosilicate system.

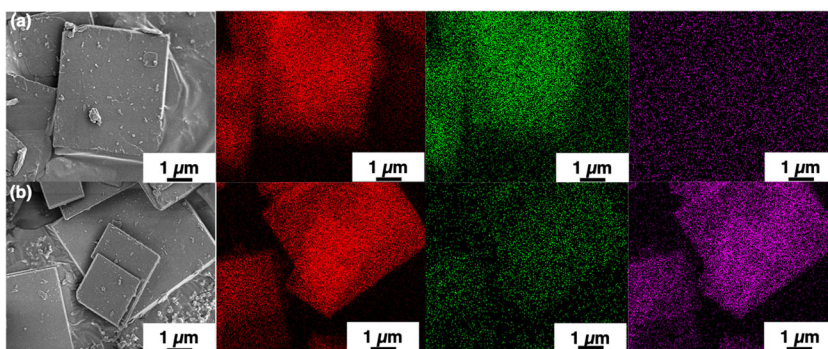


Fig. 4 SEM images and elemental mapping of octosilicate: **a** before and **b** after the reaction with a $\text{Pb}(\text{ac})_2$ solution concentration of 6.0 mM

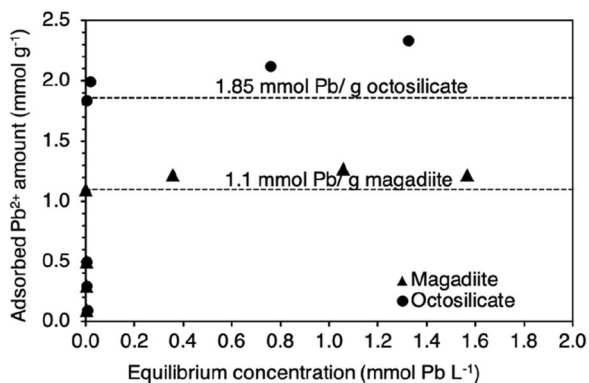


Fig. 5 Adsorption isotherms of Pb^{2+} on magadiite (triangle) and octosilicate (circle) from an aqueous solution at room temperature

After reaction for 24 h, the ranges became 5.6–9.0 for magadiite and 5.8–9.1 for octosilicate, so the proton was not exchanged with Na. The adsorption of Pb^{2+} under these conditions was 1.27 mmol/g for magadiite and 2.34 mmol/g

for octosilicate (Table 1), but from acidic solution, the amounts adsorbed decreased to 0.32 (pH 3.64) and 0.34 (pH 3.95), respectively, confirming the important role of pH.

The Langmuir model (Langmuir, 1918) was used to describe the adsorption isotherms, and the parameters are summarized in Table 2, together with the reported values. The Langmuir model is expressed as:

$$\frac{C_e}{q_e} = \frac{C_e}{q_m} + \frac{1}{q_m K_L}$$

where C_e is the equilibrium concentration (mmol/L), q_e is the amount adsorbed (mmol/g), q_m is the maximum adsorption capacity of the adsorbent (mmol/g), and K_L is the Langmuir constant (L/mmol) related to the free energy of the adsorption (ΔG). By plotting C_e/q_e (vertical axis) versus C_e (horizontal axis), the values of q_m and K_L were determined from the slope and intercept of the linear plot, respectively. The Langmuir plot (Fig. 6a) fitted magadiite with a high correlation coefficient ($R^2 = 0.9991$). The Langmuir constant (K_L), which may correlate with the ΔG value (the larger K_L value corresponded to the more negative ΔG), was high (812 L/mmol) for magadiite when compared with the

Table 1 Examples of the amounts of Pb^{2+} adsorbed on layered alkali silicates and various other ion exchangers

Adsorbents	Experimental conditions	Amount of adsorbent/solution (g/mL)	Pb^{2+} salt	Initial concentration of Pb^{2+} salt (ppm)	Amount of Pb^{2+} adsorbed (mmol Pb/g)	Reference
Natural Na-bentonite	pH < 7.0	0.0125/50	$\text{Pb}(\text{NO}_3)_2$	365	0.96	(Glatstein & Francisca, 2015)
Granular activated carbon	pH = 5.0	0.1/50	$\text{Pb}(\text{NO}_3)_2$	70	0.10	(Goel et al., 2005)
Zeolite	pH = 7.5	0.8/100	$\text{Pb}(\text{ac})_2$	20	0.012	(Jamil et al., 2010)
Carbon nanotube	pH = 5.0	0.05/100	$\text{Pb}(\text{NO}_3)_2$	14	0.072	(Li et al., 2002)
Synthetic hydroxylapatite	pH = 5.1	0.2/50	$\text{Pb}(\text{NO}_3)_2$	500	0.442	(Kaludjerovic-Radoicic & Raicevic, 2010)
Natural apatite	pH = 5.6	0.2/50	$\text{Pb}(\text{NO}_3)_2$	100	0.40	(Kaludjerovic-Radoicic & Raicevic, 2010)
Attapulgite modified with ethylenediamine	pH = 4.0	0.02/25	$\text{Pb}(\text{NO}_3)_2$	20	0.48	(Deng et al., 2013)
Magadiite	pH = 7.0	0.05/100	$\text{Pb}(\text{NO}_3)_2$	80	0.048	(Benkhatou et al., 2016)
Magadiite modified with N-(2-methoxyphenyl)-N'-(2-methylphenyl)-thiourea	pH = 7.0	0.05/100	$\text{Pb}(\text{NO}_3)_2$	80	0.096	(Benkhatou et al., 2016)
Magadiite modified with N-(2-methoxyphenyl)-N'-(2-methoxyphenyl)-thiourea	pH = 5.0	0.05/100	$\text{Pb}(\text{NO}_3)_2$	80	0.16	(Benkhatou et al., 2016)
Alginate and magadiite/di (2-ethylhexyl)phosphoric acid	pH = 4.0	0.01/10	$\text{Pb}(\text{NO}_3)_2$	1000	0.95	(Attar et al., 2019)
[$\text{C}_{22}\text{H}_{45}\text{-N}^+\text{C}_5\text{H}_8\text{N}$]-magadiite	-	0.05/100	PbCl_2	50	0.25	(Ding et al., 2018)
Magadiite	aqueous NaCl	0.08/100	$\text{Pb}(\text{NO}_3)_2$	200	0.88	(Lim et al., 2017)
Octosilicate	aqueous NaCl	0.08/200	$\text{Pb}(\text{NO}_3)_2$	200	1.5	(Lim et al., 2017)
Magadiite	pH = 6.0	0.1/50	$\text{Pb}(\text{ac})_2$	750	1.27	This study
Octosilicate	pH = 6.0	0.1/50	$\text{Pb}(\text{ac})_2$	1250	2.34	This study

Table 2 Langmuir parameters for the adsorption of Pb^{2+} on the layered alkali silicates and various other ion exchangers

Adsorbents	Initial pH	q_m (mmol/g)	K_L (L/mmol)	References
Carbon nanotubes	5.0	0.084	38	(Li et al., 2002)
Hydroxylapatite-alginate composite	5.0	1.30	18	(Googerdchian et al., 2012)
Attapulgitte modified with ethylenediamine	4.0	1.25	11	(Deng et al., 2013)
Magadiite	7.0	0.048–0.096	0.04–0.098	(Benkhatou et al., 2016)
Magadiite	4.0	0.95	0.0055	(Attar et al., 2019)
Magadiite in NaCl	–	0.97	9.8	(Lim et al., 2017)
Magadiite	6.0	1.23	812	This study
Octosilicate	6.0	2.32	51	This study

previous studies (Benkhatou et al., 2016; Lim et al., 2017; Attar et al., 2019), suggesting the high affinity between the silicate surface and Pb^{2+} ions.

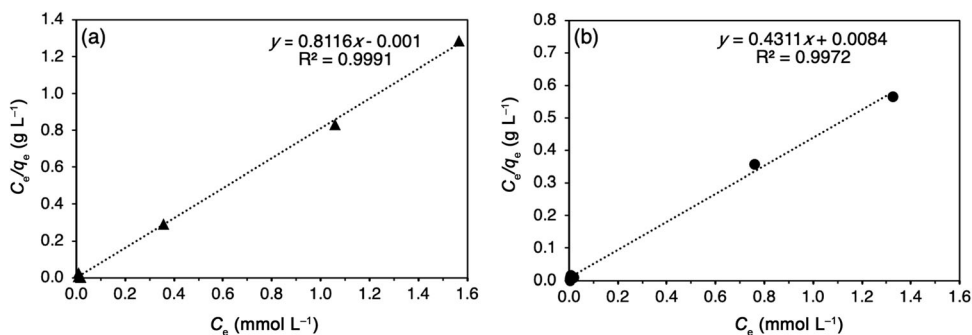
In the case of octosilicate, the Langmuir model was fitted with a high correlation coefficient ($R^2 = 0.9972$) at concentrations between 0.6 and 6.0 mM (Fig. 6b). The deviation of the plot from the Langmuir model at concentrations of <0.6 mM has not been explained clearly thus far; the precipitation of Pb salt may have contributed to the change in the concentration of Pb^{2+} . In order to discuss the point, the precipitation of Pb^{2+} salts was proposed as a mechanism for collection of Pb^{2+} , in addition to the cation exchange. Precipitation of Pb salts may occur as a result of the change in pH caused by ion exchange. The Na released from the layered silicates caused an increase in pH as mentioned above; the pH of the $\text{Pb}(\text{ac})_2$ solution was in the range 5.9–6.0, while that of the suspension after the reactions between the Pb^{2+} and the layered silicates was in the range 5.6–9.0 for magadiite and 5.8–9.1 for octosilicate. The precipitation of $\text{Pb}_2(\text{OH})\text{Cl}_3$ during the reaction between magadiite and $\text{Pb}(\text{II})$ nitrate in aqueous NaCl solution was reported by Lim et al. (2017). The precipitation of $\text{In}(\text{OH})_3$ during the reaction between layered alkali titanates and $\text{In}(\text{III})$ chloride in water was reported by Sirinakorn et al. (2018b) and the precipitation of cadmium carbonate ($\text{Cd}(\text{CO}_3)_2$) during the reaction between layered alkali titanates and $\text{Cd}(\text{II})$ acetate in water was reported by Sirinakorn et al. (2019). $\text{Pb}(\text{OH})_2$ precipitates from water at a pH of

>6.5 (Baes & Mesmer, 1976) and PbCO_3 precipitates from water at $\text{pH} < 9.5$ (Taylor & Lopata, 1984). The solubility product constants (K_{sp}) of $\text{Pb}(\text{OH})_2$ and PbCO_3 are 1.2×10^{-15} and 7.4×10^{-14} , respectively. In the present study, the pH of the suspension after the adsorption experiment was 5.6–9.0 for magadiite and 5.8–9.1 for octosilicate, so that the precipitation of $\text{Pb}(\text{OH})_2$ and/or PbCO_3 was a plausible mechanism for the amount of Pb^{2+} adsorbed above the value of the CEC, especially in the case of octosilicate. The complicated Langmuir plot supported the hypothesis that the removal of Pb^{2+} by the reaction with octosilicate involved ion exchange and the precipitation of Pb salts.

Scanning electron microscopy images of magadiite and octosilicate before and after reaction with $\text{Pb}(\text{ac})_2$ solution of 4.0 mM for magadiite and 6.0 mM for octosilicate are shown in Fig. 7. Irregularly shaped particles <100 nm wide were observed on the edge surface of the silicate particles (Fig. 7b,d). The particles were thought to be $\text{Pb}(\text{OH})_2$ and/or PbCO_3 , though crystalline $\text{Pb}(\text{OH})_2$ and PbCO_3 were not detected in the XRD patterns (Figs 1, 2) and showing the absence of Si in the small particles by SEM/EDX analyses was not possible.

Kinetics of Adsorption of Pb^{2+} on Magadiite and Octosilicate

Pb^{2+} adsorption on magadiite reached equilibrium within 5 min, while the adsorption of Pb^{2+} on octosilicate took 60 min to reach equilibrium. The reaction time reported for the adsorption of Pb^{2+} on magnetite (Hong et al., 2020), hydroxylapatite

**Fig. 6** Langmuir plots of the adsorption of Pb^{2+} onto **a** magadiite (triangles) and **b** octosilicate (circles)

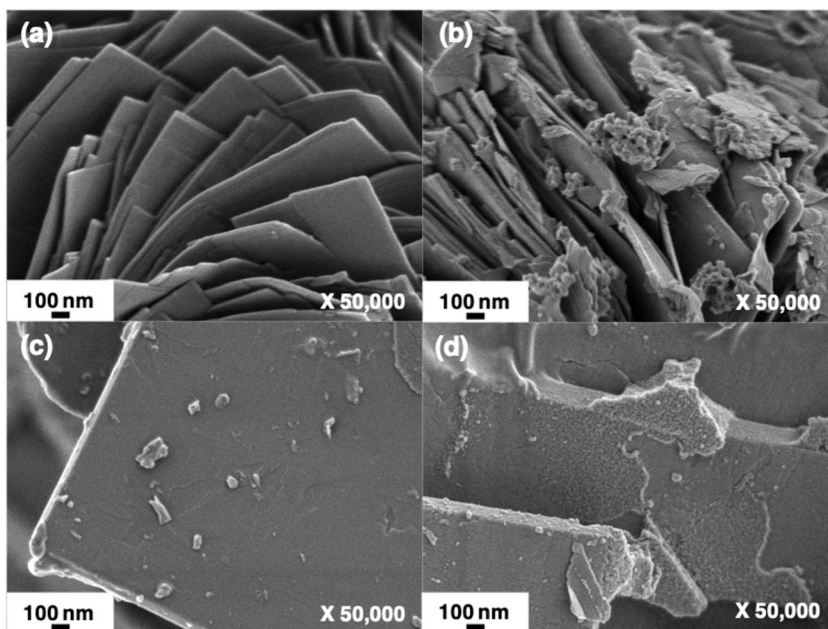


Fig. 7 SEM images of **a** magadiite and **c** octosilicate before and after the reaction with $\text{Pb}(\text{ac})_2$ solution at a concentration of **b** 4.0 mM for magadiite and **d** 6.0 mM for octosilicate

(Dong et al., 2010; Googerdchian et al., 2012; Choudhury et al., 2015), ferroxane (Moattari et al., 2015), attapulgite (Deng et al., 2013), and carbon nanotubes (Wang et al., 2007; Kabbashi et al., 2009; Robati, 2013) are summarized in Table 3. The short reaction time (5 min) for the removal of Pb^{2+} is an advantage of magadiite as an adsorbent. The particle morphology (platy

particles a few μm wide for octosilicate and flower-like aggregates of platy particles 1–2 μm across for magadiite) affected the reaction time; the flower-like aggregates of magadiite particles were suitable for smooth diffusion of Pb^{2+} . This characteristic is worthy of further investigation for the adsorption of various metal ions on magadiite.

Table 3 Examples of the kinetics of adsorption of Pb^{2+} on various ion exchangers

Adsorbents	Amount of adsorbent/solution (g/mL)	Initial pH	Initial concentration (ppm)	Amount of Pb^{2+} adsorbed (q_e) (mmol Pb/g)	Time to reach equilibrium for Pb^{2+} adsorption (min)	References
Carbon nanotube	0.005/250	5.0	20	0.1814	80	(Kabbashi et al., 2009)
Carbon nanotube	0.010/250	5.0	40	0.0904	80	(Kabbashi et al., 2009)
Hydroxylapatite	0.075/30	5.0	900	0.93	240	(Googerdchian et al., 2012)
Ferroxane	0.141/25	6.3	5	0.017	180	(Moattari et al., 2015)
Attapulgite modified with ethylenediamine	0.03/25	5.5	20	0.078	100	(Deng et al., 2013)
Magadiite	0.05/50	7.0	100	0.188	60	(Benkhatou et al., 2016)
Magadiite	0.1/10	4.0	50	0.024	180	(Attar et al., 2019)
Magadiite	0.1/50	6.0	455	1.10	5	This study
Octosilicate	0.1/50	6.0	767	1.84	60	This study

CONCLUSIONS

Magadiite and octosilicate concentrated Pb^{2+} from aqueous solution at room temperature (25°C) under pH 6.0. The maximum amounts of Pb^{2+} adsorbed were 1.27 mmol Pb/g magadiite and 2.34 mmol Pb/g octosilicate, which were greater than the theoretical CEC values (2.2 meq/g for magadiite, 3.7 meq/g for octosilicate), suggesting the mechanisms of ion exchange and precipitation. The amounts of Pb^{2+} adsorbed on magadiite and octosilicate were large when compared with previous reports (carbon nanotube, activated carbon, fly ash, and clay minerals), confirming high-capacity adsorption of Pb^{2+} from aqueous solution by magadiite and octosilicate. Pb^{2+} adsorption reached equilibrium within 5 min for magadiite, another advantage for the collection of Pb^{2+} from water.

ACKNOWLEDGMENTS

This work was supported by a Research Chair Grant 2017 (Grant FDA-CO-2560-5655) from the National Science and Technology Development Agency (NSTDA), Thailand and the Program Management Unit for Human Resources & Institutional Development, Research and Innovation, NXPO (Grant number B05F630117), Thailand. Two of the authors (D.A.S. and T.T.S.) acknowledge the Vidyasirimedhi Institute of Science and Technology for a scholarship for their PhD studies.

FUNDING

Funding sources are as stated in the Acknowledgments.

DECLARATIONS

Conflict of Interest

The authors declare that they have no conflict of interest.

REFERENCES

- Abbas, A., Al-Amer, A. M., Laoui, T., Al-Marri, M. J., Nasser, M. S., Khraish, M., & Atieh, M. A. (2016). Heavy metal removal from aqueous solution by advanced carbon nanotubes: critical review of adsorption applications. *Separation and Purification Technology*, *157*, 141–161.
- Al-Zboon, K., Al-Harash, M. S., & Hani, F. B. (2011). Fly ash-based geopolymer for Pb removal from aqueous solution. *Journal of Hazardous Materials*, *188*(1-3), 414–421.
- Aliyu, A., Kariim, I., & Abdulkareem, S. A. (2017). Effects of aspect ratio of multi-walled carbon nanotubes on coal washery waste water treatment. *Journal of Environmental Management*, *202*, 84–93.
- Attar, K., Demey, H., Bouazza, D., & Sastre, A. M. (2019). Sorption and desorption studies of Pb (II) and Ni (II) from aqueous solutions by a new composite based on alginate and magadiite materials. *Polymers*, *11*(2), 340–358.
- Auerbach, S. M., Carrado, K. A., & Dutta, P. K. (2004). *Handbook of Layered Materials*. CRC Press, Boca Raton, Florida, USA.
- Baes, C., & Mesmer, R. (1976). *The Hydrolysis of Cations*. Wiley, Hoboken, New Jersey, USA.
- Barbosa, R., Lapa, N., Lopes, H., Gunther, A., Dias, D., & Mendes, B. (2014). Biomass fly ashes as low-cost chemical agents for Pb removal from synthetic and industrial wastewaters. *Journal of Colloid and Interface Science*, *424*, 27–36.
- Benkhatou, S., Djelad, A., Sassi, M., Bouchekara, M., & Bengueddach, A. (2016). Lead (II) removal from aqueous solutions by organic thiourea derivatives intercalated magadiite. *Desalination and Water Treatment*, *57*(20), 9383–9395.
- Chen, Q., Luo, Z., Hills, C., Xue, G., & Tyrer, M. (2009). Precipitation of heavy metals from wastewater using simulated flue gas: Sequent additions of fly ash, lime and carbon dioxide. *Water Research*, *43*(10), 2605–2614.
- Chen, W. F., Pan, L., Chen, L. F., Yu, Z., Wang, Q., & Yan, C. C. (2014). Comparison of EDTA and SDS as potential surface impregnation agents for lead adsorption by activated carbon. *Applied Surface Science*, *309*, 38–45.
- Choudhury, P. R., Mondal, P., & Majumdar, S. (2015). Synthesis of bentonite clay based hydroxyapatite nanocomposites cross-linked by glutaraldehyde and optimization by response surface methodology for lead removal from aqueous solution. *RSC Advances*, *5*(122), 100838–100848.
- Clearfield, A. (1996). *Comprehensive Supramolecular Chemistry, Vol. 7, Solid-State Supramolecular Chemistry: Two- and Three-Dimensional Inorganic Networks* (G. Alberti and T. Bein, editors). Pergamon.
- Dąbrowski, A., Hubicki, Z., Podkościelny, P., & Robens, E. (2004). Selective removal of the heavy metal ions from waters and industrial wastewaters by ion-exchange method. *Chemosphere*, *56*(2), 91–106.
- Deng, Y., Gao, Z., Liu, B., Hu, X., Wei, Z., & Sun, C. (2013). Selective removal of lead from aqueous solutions by ethylenediamine-modified attapulgite. *Chemical Engineering Journal*, *223*, 91–98.
- Ding, H., Chen, Y., Fu, T., Bai, P., & Guo, X. (2018). Nanosheet-based magadiite: a controllable two-dimensional trap for selective capture of heavy metals. *Journal of Materials Chemistry A*, *6*(28), 13624–13632.
- Divrikli, U., Kartal, A. A., Soylak, M., & Elci, L. (2007). Preconcentration of Pb(II), Cr(III), Cu(II), Ni(II) and Cd(II) ions in environmental samples by membrane filtration prior to their flame atomic absorption spectrometric determinations. *Journal of Hazardous Materials*, *145*(3), 459–464.
- Dong, L., Zhu, Z., Qiu, Y., & Zhao, J. (2010). Removal of lead from aqueous solution by hydroxyapatite/magnetite composite adsorbent. *Chemical Engineering Journal*, *165*(3), 827–834.
- Endo, K., Sugahara, Y., & Kuroda, K. (1994). Formation of intercalation compounds of a layered sodium octosilicate with n-alkyltrimethylammonium ions and the application to organic derivatization. *Bulletin of the Chemical Society of Japan*, *67*(12), 3352–3355.
- Giles, C., MacEwan, T., Nakhwa, S., & Smith, D. (1960). A system of classification of solution adsorption isotherms, and its use in diagnosis of adsorption mechanisms and in measurement of specific surface areas of solids. *Journal of the Chemical Society*, *111*, 3973–3993.
- Glatstein, D. A., & Francisca, F. M. (2015). Influence of pH and ionic strength on Cd, Cu and Pb removal from water by adsorption in Na-bentonite. *Applied Clay Science*, *118*, 61–67.
- Goel, J., Kadirvelu, K., Rajagopal, C., & Garg, V. K. (2005). Removal of lead(II) by adsorption using treated granular activated carbon: batch and column studies. *Journal of Hazardous Materials*, *125*(1-3), 211220.
- Googerdchian, F., Moheb, A., & Emadi, R. (2012). Lead sorption properties of nanohydroxyapatite-alginate composite adsorbents. *Chemical Engineering Journal*, *200-202*, 471–479.
- Guerra, D. L., Pinto, A. A., Airoldi, C., & Viana, R. R. (2008). Adsorption of arsenic(III) into modified lamellar Na-magadiite in aqueous medium—Thermodynamic of adsorption process. *Journal of Solid State Chemistry*, *181*(12), 3374–3379.
- Guerra, D. L., Ferreira, J. N., Pereira, M. J., Viana, R. R., & Airoldi, C. (2010). Use of natural and modified magadiite as adsorbents to remove Th(IV), U(VI), and Eu(III) from aqueous media—Thermodynamic and equilibrium study. *Clays and Clay Minerals*, *58*(3), 327–339.
- Hatsushika, T. (1996). Ion-exchange characteristics of magadiite for divalent metallic ions. *Inorganic Materials*, *3*, 319–326.

- Homhuan, N., Bureekaew, S., & Ogawa, M. (2017a). Efficient concentration of Indium(III) from aqueous solution using layered silicates. *Langmuir*, 33(38), 9558–9564.
- Homhuan, N., Imwiset, K., Sirinakorn, T., Bureekaew, S., & Ogawa, M. (2017b). Ion exchange of a layered alkali silicate, magadiite, with metal ions. *Clay Science*, 21(2), 21–28.
- Hong, J., Xie, J., Mirshahghassemi, S., & Lead, J. (2020). Metal (Cd, Cr, Ni, Pb) removal from environmentally relevant waters using polyvinylpyrrolidone-coated magnetite nanoparticles. *RSC Advances*, 10(6), 3266–3276.
- Ide, Y., & Ogawa, M. (2007). Efficient way to attach organosilyl groups in the interlayer space of layered solids. *Bulletin of the Chemical Society of Japan*, 80(8), 1624–1629.
- Ide, Y., Ochi, N., & Ogawa, M. (2011). Effective and selective adsorption of Zn^{2+} from seawater on a layered silicate. *Angewandte Chemie International Edition*, 50(3), 654–656.
- Ide, Y., Sadakane, M., Sano, T., & Ogawa, M. (2014). Functionalization of layered titanates. *Journal of Nanoscience and Nanotechnology*, 14(3), 2135–2147.
- Jamil, T. S., Ibrahim, H. S., Abd El-Maksoud, I. H., & El-Wakeel, S. T. (2010). Application of zeolite prepared from Egyptian kaolin for removal of heavy metals: I. Optimum conditions. *Desalination*, 258(1–3), 34–40.
- Jiang, J., Liang, D., & Zhong, Q. (2011). Precipitation of indium using sodium tripolyphosphate. *Hydrometallurgy*, 106(3–4), 165–169.
- Kabbashi, N. A., Ateih, M. A., Al-Mamun, A., Mirghami, M. E., Alam, M., & Yahya, N. (2009). Kinetic adsorption of application of carbon nanotubes for Pb(II) removal from aqueous solution. *Journal of Environmental Sciences*, 21(4), 539–544.
- Kaludjerovic-Radoicic, T., & Raicevic, S. (2010). Aqueous Pb sorption by synthetic and natural apatite: Kinetics, equilibrium and thermodynamic studies. *Chemical Engineering Journal*, 160(2), 503–510.
- Kaneko, S., & Ogawa, M. (2013). Effective concentration of dichromate anions using layered double hydroxides from acidic solutions. *Applied Clay Science*, 75, 109–113.
- Komatsu, Y., Fujiki, Y., & Sasaki, T. (1982). Ion exchange equilibrium of alkali metal ions between crystalline hydrous titanium dioxide fibers and aqueous solution. *Bunseki Kagaku*, 31(7), 225–229.
- Kosuge, K., Yamazaki, A., Tsunashima, A., & Otsuka, R. (1992). Hydrothermal synthesis of magadiite and kenyaite. *Nippon Seramikkusu Kyokai Gakujutsu Ronbunshi*, 100, 326–331.
- Lagaly, G., Beneke, K., & Weiss, A. (1975). Magadiite and H-magadiite. I. Sodium magadiite and some of its derivatives. *American Mineralogist*, 60(7–8), 642–649.
- Langmuir, I. (1918). The adsorption of gases on plane surfaces of glass, mica and platinum. *Journal of the American Chemical Society*, 40(9), 1361–1403.
- Li, Y.-H., Wang, S., Wei, J., Zhang, X., Xu, C., Luan, Z., Wu, D., & Wei, B. (2002). Lead adsorption on carbon nanotubes. *Chemical Physics Letters*, 357(3,4), 263–266.
- Lim, W. T., Jang, J.-H., Park, N.-Y., Paek, S.-M., Kim, W.-C., & Park, M. (2017). Spontaneous nanoparticle formation coupled with selective adsorption in magadiite. *Journal of Materials Chemistry A*, 5(8), 4144–4149.
- Liu, Y., Yan, C., Zhang, Z., Wang, H., Zhou, S., & Zhou, W. (2016). A comparative study on fly ash, geopolymer and faujasite block for Pb removal from aqueous solution. *Fuel*, 185, 181–189.
- Mandel, K., Drenkova-Tuhtan, A., Hutter, F., Gellermann, C., Steinmetz, H., & SEXTL, G. (2013). Layered double hydroxide ion exchangers on superparamagnetic microparticles for recovery of phosphate from waste water. *Journal of Materials Chemistry A*, 1(5), 1840–1848.
- Miyata, S. (1983). Anion-exchange properties of hydroxalcalite-like compounds. *Clays and Clay Minerals*, 31(4), 305–311.
- Mizukami, N., Tsujimura, M., Kuroda, K., & Ogawa, M. (2002). Preparation and characterization of Eu-magadiite intercalation compounds. *Clays and Clay Minerals*, 50(6), 799–806.
- Moattari, R. M., Rahimi, S., Rajabi, L., Derakhshan, A. A., & Keyhani, M. (2015). Statistical investigation of lead removal with various functionalized carboxylate ferroxane nanoparticles. *Journal of Hazardous Materials*, 283, 276–291.
- Mokhtar, A., Medjhoua, Z. A. K., Djelad, A., Boudia, A., Bengueddach, A., & Sassi, M. (2018). Structure and intercalation behavior of copper (II) on the layered sodium silicate magadiite material. *Chemical Papers*, 72(1), 39–50.
- Mousa, N. E., Simonescu, C. M., Patescu, R.-E., Onose, C., Tardei, C., Culita, D. C., Oprea, O., Patroi, D., & Lavric, V. (2016). Pb^{2+} removal from aqueous synthetic solutions by calcium alginate and chitosan coated calcium alginate. *Reactive and Functional Polymers*, 109, 137–150.
- Murakami, Y., Nanba, M., Tagashira, S., & Sasaki, Y. (2006). Ion-exchange and structural properties of magadiite. *Clay Science*, 12, 37–41.
- Ogawa, M., & Takahashi, Y. (2007). Preparation and thermal decomposition of Co(II)-magadiite intercalation compounds. *Clay Science*, 13(4–5), 133–138.
- Okada, T., Seki, Y., & Ogawa, M. (2014). Designed nanostructures of clay for controlled adsorption of organic compounds. *Journal of Nanoscience and Nanotechnology*, 14(3), 2121–2134.
- Otunola, B. O., & Ololade, O. O. (2020). A review on the application of clay minerals as heavy metal adsorbents for remediation purposes. *Environmental Technology and Innovation*, 100692.
- Robati, D. (2013). Pseudo-second-order kinetic equations for modeling adsorption systems for removal of lead ions using multi-walled carbon nanotube. *Journal of Nanostructure in Chemistry*, 3(1), 55.
- Rojo, J. M., Ruiz-Hitzky, E., & Sanz, J. (1988). Proton-sodium exchange in magadiite. spectroscopic study (NMR, IR) of the evolution of interlayer OH groups. *Inorganic Chemistry*, 27(16), 2785–2790.
- Schwieger, W., Lagaly, G., Auerbach, S., Carrado, K., & Dutta, P. (2004). *Handbook of Layered Materials*. Marcel Dekker, Inc., New York.
- Selvam, T., Inayat, A., & Schwieger, W. (2014). Reactivity and applications of layered silicates and layered double hydroxides. *Dalton Transactions*, 43(27), 10365–10387.
- Sirinakorn, T., Imwiset, K., Bureekaew, S., & Ogawa, M. (2018a). Inorganic modification of layered silicates toward functional inorganic-inorganic hybrids. *Applied Clay Science*, 153, 187–197.
- Sirinakorn, T., Bureekaew, S., & Ogawa, M. (2018b). Highly efficient Indium (III) collection from water by a reaction with a layered titanate ($Na_2Ti_3O_7$). *European Journal of Inorganic Chemistry*, 2018(34), 3835–3839.
- Sirinakorn, T., Bureekaew, S., & Ogawa, M. (2019). Layered titanates ($Na_2Ti_3O_7$ and $Cs_2Ti_5O_{11}$) as very high capacity adsorbents of Cadmium (II). *Bulletin of the Chemical Society of Japan*, 92(1), 16.
- Taylor, P., & Lopata, V. J. (1984). Stability and solubility relationships between some solids in the system $PbO-CO_2-H_2O$. *Canadian Journal of Chemistry*, 62(3), 395–402.
- Vortmann, S., Rius, J., Siegmann, S., & Gies, H. (1997). Ab initio structure solution from X-ray powder data at moderate resolution: crystal structure of a microporous layer silicate. *The Journal of Physical Chemistry B*, 101(8), 1292–1297.
- Wang, H., Zhou, A., Peng, F., Yu, H., & Yang, J. (2007). Mechanism study on adsorption of acidified multiwalled carbon nanotubes to Pb (II). *Journal of Colloid and Interface Science*, 316(2), 277–283.

(Received 26 August 2020; revised 28 May 2021; AE: Binoy Sarkar)